

# $\alpha$ and $\beta$ forms of oxalic acid di-hydrate at high pressure: a theoretical simulation and a neutron diffraction study

Piero Macchi,<sup>\*a</sup> Nicola Casati,<sup>\*b</sup> William G. Marshall<sup>c</sup> and Angelo Sironi<sup>d</sup>

Received (in XXX, XXX) Xth XXXXXXXXX 200X, Accepted Xth XXXXXXXXX 200X

First published on the web Xth XXXXXXXXX 200X

DOI: 10.1039/b000000x

The high pressure structure of  $\alpha$ -oxalic acid di-hydrate shows a prototypical behaviour of acid to base proton transfer reaction. The solid state transformation has been characterized by neutron and X-ray diffraction as well as by quantum chemical calculations with periodic boundary conditions. The two resonant configurations playing the most important role in the hydrogen bond mechanism, *i.e.* a neutral and a charge transfer configuration, are interchanged by modifying the pressure on the system. A different behaviour is predicted for the less common  $\beta$  form, despite an apparently similar packing motif. Implications for the characterization of hydrogen bonds in the solid state are discussed as well as the possibility of estimating internal energy variations from experimental measurements.

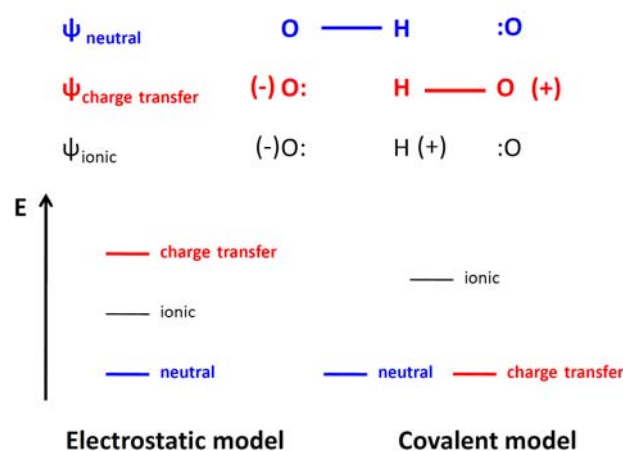
## Introduction

The hydrogen bond (HB) is crucial in many aspects of chemistry, ranging from biochemistry to material science; however it is still one of the most debated interactions. Its “discovery”<sup>1,2</sup> was mainly due to the experimental evidence of so-called hydrogen bridges.<sup>3</sup> The nature of this bond, however, remained quite puzzling for some time. Pauling dedicated to the HB a large chapter of his famous *The nature of the chemical bond*,<sup>4</sup> anticipating some arguments of a valence bond (VB) treatment of this interaction, although for many years the HB was considered simply as electrostatic.

There is nowadays quite a consensus that weak HB's, characterized by long distances, do not contain covalent character, whereas strong HB's (*i.e.* short hydrogen bridges) are more controversial. A classification and rationalization of strong HB's was presented by Gilli,<sup>5</sup> who proposed that only three types of HB's may have large covalency and therefore a strong character: the *resonance assisted* and the *positive* or *negative charge assisted* HB's. These three classes are tightly connected to the very same interpretative scheme, grounded on a VB idea (see scheme 1): if the two covalent resonant structures of a D-H---A HB system are close enough in energy, then their mixing will be large and both D-H and H-A bonds will be partially covalent (here, D and A are the HB donor and acceptor, respectively). An important corollary of this theory is that a single minimum, symmetric hydrogen position would be expected in symmetric adducts connected by strong HBs, instead of a disordered double minimum. Madsen *et al.*,<sup>6</sup> however, noted an interesting isotopic effect in the low barrier hydrogen bonds of benzoylacetone, where deuterated species show a bimodal probability density function, whereas hydrogenated species have sufficient energy to overwhelm the low barrier, showing a unimodal distribution.

As from scheme 1, a strong HB requires that a charge transfer (CT) configuration be sufficiently close in energy to be

“resonant” with the neutral (N) configuration. The CT implies also a proton transfer from the HB donor to the HB acceptor and this is favoured by a positive charge on the donor and/or a negative charge on the acceptor. A CT configuration shall not be confused with an electrostatic treatment of the HB (scheme 1, left), which holds only in the absence of CT/N resonance and it is favoured by the mixing of a neutral and an ionic configuration (defined as in scheme 1).



**Scheme 1.** The relative energy order of Coulson's three VB resonance forms describing H-bond in an O-H...O system, in the electrostatic (left) and covalent case (right). This scheme summarizes conclusions by Gilli.<sup>5</sup>

Some exceptions to the classification by Gilli are possible if, for example, the HB acceptor, albeit neutral, is extremely polar or polarisable and therefore its proton affinity is sufficiently high. One such molecule is certainly water, which is in fact known to accept quite strong HBs in the solid state. In this context, a prototypical species is the oxalic acid di-hydrate, **1** (see Figure 1), where a strong HB aggregation occurs between H<sub>2</sub>C<sub>2</sub>O<sub>4</sub> and two H<sub>2</sub>O molecules.

The crystallo-chemical studies on oxalic acid are quite numerous and date back to 1880.<sup>7,8</sup> Two anhydrous (**2a** and **2b**) and two di-hydrated forms (**1a** and **1b**) are known and have been studied over the years. Interestingly, the first crystal structure determinations<sup>9</sup> of **1a** using X-ray diffraction techniques, were carried out to ascertain whether H<sub>2</sub>C<sub>2</sub>O<sub>4</sub> and H<sub>2</sub>O or otherwise [C<sub>2</sub>O<sub>4</sub>]<sup>2-</sup> and H<sub>3</sub>O<sup>+</sup> species are actually present in the solid state. However, the low quality of those experiments did not resolve the debate until the more accurate data, and a structural refinement of the heavier atom positions, were published by Ahmed and Cruickshank,<sup>10</sup> who undoubtedly demonstrated that the crystal is composed of neutral species. Despite the absence of information concerning the H atom positions, their key argument was based on the C-O distances, clearly indicating the presence of single and double bonds as expected in the oxalic acid but at variance from the oxalate anion. Quite a number of neutron diffraction studies were carried out on **1a** in deuterated form, affected by a small isotopic effect. These neutron studies<sup>11</sup> confirmed Cruickshank's structural model, but also demonstrated the quite elongated O-H distance in the oxalic acid, indicating a strong HB in agreement with the very short O---O separation. Variable temperature experiments<sup>12</sup> also proved that the HB distance is somewhat dependent on the crystal packing, with a small but significant O---O shortening and O-H elongation at low T.

During a nuclear magnetic resonance experiment of the deuterated isotopomer, a new form (**1b**) was identified and structurally characterized.<sup>13</sup> To the best of our knowledge, all structural identifications of this form have been carried out on the deuterated species. An intriguing remark by Coppens and Sabine<sup>11c</sup> suggests that the deuterated **1a** form might be a sort of disappearing polymorph as Craven *et al.*<sup>11</sup> were unable to obtain **1a** after **1b** was grown. However, there was no other evidence of this in the 40 years of research afterwards. Moreover, as discussed in the experimental section, we could isolate the deuterated **1a** polymorph even after having incidentally grown **1b**.

In the CSD,<sup>14</sup> about 100 structures are deposited containing oxalic acid co-crystallized with other molecules or ions, some of them showing the same aggregation as in the oxalic acid dihydrate. Form **1a** is definitely the most investigated phase (with more than 30 structures in CSD), however many other interesting structures have been reported. Recently, Wenger and Bernstein<sup>15</sup> reported two unprecedented forms of oxalic acid sesqui-hydrate. In both polymorphs, hydronium cations were found and consequently hydrogen oxalate molecules were identified.

In recent years, structural characterizations of hydrogen bonded molecular crystals under high pressure have been published,<sup>16</sup> whereas much fewer number of studies were instead devoted to investigate the structural features of HB systems under pressure from a quantum mechanical point of view.

Oxalic acid di-hydrate has been the subject of some high pressure investigations. Putkonen *et al.*<sup>17</sup> investigated the equation of state of **1a** up to 0.5 GPa, but no special change was observed. Marshall *et al.*<sup>18</sup> reported high pressure

experiments on **1a** and **2a**. The aim of that study was searching possible pressure dependent phase transitions (for example, **1a** → **1b**), which were not observed for both species, at least up to 3 GPa. On the other hand, as we have recently reported,<sup>19</sup> above 4 GPa **1a** transforms into a proton transfer phase forming ionic moieties. This conclusion came from careful single crystal X-ray diffraction experiments and preliminary theoretical simulations. After this study, we have carried out multi-pressure neutron powder diffraction experiments on **1a** to validate the previous conclusions. These new results are reported here, together with a full theoretical comparison between the **1a** and **1b** forms in the range 0-10 GPa.

## Experimental section

### Neutron diffraction study at high pressure

Deuterated samples of **1a**, suitable for neutron diffraction experiments, were grown from slow evaporation of deuterated aqueous solution, after three cycles of deuteration. A preliminary high temperature and rapid evaporation gave a mixed phase with excess of **1b** form, but the subsequent re-crystallizations produced the expected **1a**.

Ambient-temperature, high-pressure neutron powder diffraction data were collected by the time-of-flight technique at the PEARL beamline high-pressure facility (HiPr) at the ISIS spallation neutron source. Approximately 50 mm<sup>3</sup> of perdeuterated oxalic acid di-hydrate was gently ground into a fine powder and loaded into a standard null scattering capsule gasket.<sup>20</sup> A small pellet of lead was added to the centre of the sample to act as a suitable pressure marker using the known equation of state<sup>21</sup> and a 1:1 mixture of perdeuterated pentane and isopentane was used as the pressure transmitting medium. The usual preferred 4:1 mixture of methanol and ethanol was not used as previous experiments<sup>18</sup> indicated this medium reacts with the sample (esterification) at pressures beyond ~1 GPa.

The filled gasket assembly was then loaded into a type V3 Paris–Edinburgh (P–E) high pressure cell using standard profile WC anvils. The hydraulic pressure within the P–E cell ram was monitored and controlled by means of a computer-controlled hydraulic system.

Time-of-flight neutron powder diffraction data suitable for structure refinement were obtained by electronically focusing the 1080 individual detector element spectra of the main 2θ = 90° detector bank. The summed pattern was then normalized with respect to the incident beam monitor and the corrected scattering from a standard vanadium calibration sample. Lastly, the diffraction pattern intensities were corrected for the wavelength and scattering-angle dependence of the neutron attenuation by the P–E cell anvil (WC) and gasket (TiZr) materials.

Sixteen data sets were collected up to an maximum applied load of 79 tonnes, which corresponded to a sample pressure of 7.6 GPa. At each point, unit cell parameters were refined together with the pressure marker, using the software TOPAS.<sup>22</sup> Longer duration data collection runs were obtained at 1.81, 4.33 and 6.16 GPa and these were used to carry out full structural refinements. Above 7 GPa the hydrostatic

behaviour of the pressure transmitting liquid is lost,<sup>23</sup> data were anyway collected up to 7.6 GPa but only unit cell constants were refined.

### 5 Ab initio quantum mechanical simulations

The phases  $\alpha$  and  $\beta$  of oxalic acid dihydrate were simulated at different pressure regimes by means of density functional calculations under periodic boundary conditions. The code CRYSTAL09<sup>24</sup> was used, adopting a B3LYP<sup>25</sup> functional and a 6-31(2d, 2p) basis set type. To avoid divergence problems, a “level shifting” was applied to avoid coupling of occupied and unoccupied Kohn-Sham orbitals (0.4 Hartree) and at the end of each cycle a partial mixing of the Kohn-Sham matrix with that of the previous cycle (20%), in order to avoid instability of the wave function (otherwise oscillating between conducting and dielectric states when higher compression is simulated).<sup>5</sup>

Smaller size basis sets, like 3-21G, were found to be inadequate because optimizing too small unit cell volumes.

When simulating solid state phases of molecular crystals, some problems may arise in the low compression regime, because of the poor description of dispersive forces, which are the major sources of cohesion in many neutral non-polar molecular crystals under ambient conditions. However, for oxalic acid di-hydrate this problem is negligible, by virtue of the strong polar HB's, that make the intermolecular interactions quite tight even at room pressure. The empirical description of dispersive forces implemented with a Grimme scheme<sup>26</sup> was tested, but a substantial re-parameterization was necessary in the presence of such strong HB, otherwise unit cell volumes were substantially underestimated. Thus, the B3LYP functional, without any dispersion correction, appeared as the best approximation. As demonstrated below, the agreement between neutron diffraction results and theoretical calculations is quite good.

The geometry optimisations were carried out by minimizing the pseudo-enthalpy function  $E_{el} + PV$ . Frequencies were computed at the  $\Gamma$  point of the Brillouin zone and Gibbs free energy (G) was therefore computed, which allow to see the effect of temperature or different isotopes on the relative stabilities of the two phases.

A useful tool to visualize differences or similarities between geometries of molecules or aggregates in the solid state is provided by the Hirshfeld surfaces analysis. The Hirshfeld surface of a molecule in a crystal is uniquely defined and it contains the portion of space in which the promolecule electron density contributes more than 50% of the total procrystal electron density.<sup>8</sup> Spackman and co-workers<sup>27</sup> analysed the distribution of internal ( $d_i$ ) and external ( $d_e$ ) distances from the molecular surface, an approach particularly useful for emphasising the diversities between polymorphs or the similarities between isomorphs. For this reason, this method has also been adopted to visualise the evolution of a crystal structure on increasing the pressure.<sup>28</sup> The software Crystal Explorer was used.<sup>29</sup>

## Results and discussion

At variance with the two anhydrous forms, the two dihydrated polymorphs of oxalic acid are characterized by similar supra-molecular motifs, based on the HB aggregation between one oxalic acid (donor) and two waters (acceptor), which we will call **HB1** hereinafter, see atoms represented as balls in Figure 1. Within the first coordination sphere, the main difference is the orientation of the two HB receiving waters: in **1 $\alpha$** , one of the oxygen lone pairs is directed toward the oxalic proton, thus making the perfect angle to form a strong HB; in **1 $\beta$** , the oxalic proton is almost bisecting the oxygen lone pairs. This discrepancy produces a completely different packing in the second coordination sphere, making the two polymorphs quite different.

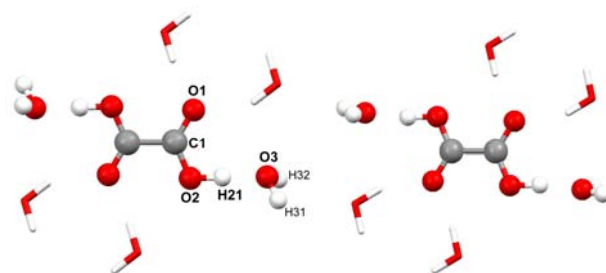


**Figure 1** Room pressure simulations of the neutral configuration of **1 $\alpha$**  (left) and **1 $\beta$**  (right). The oxalic acid and the two HB receiving waters belong to the **HB1** aggregate and their atoms are represented as balls. The atom labelling scheme is also displayed.

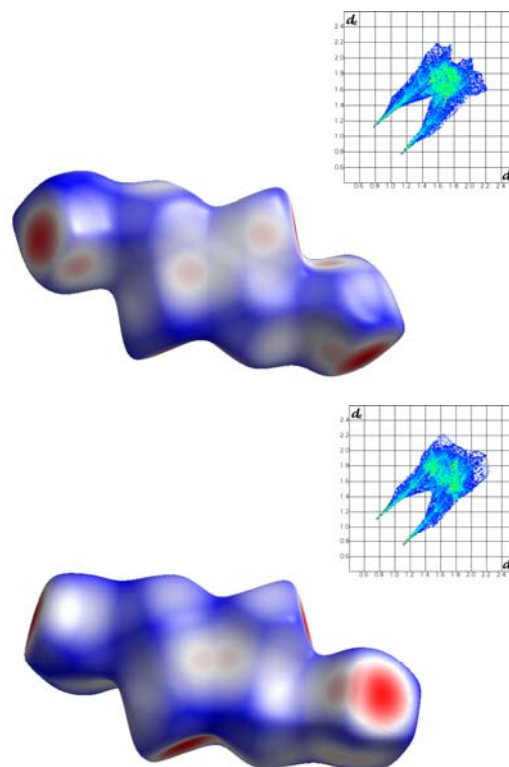


**Figure 2** Hirshfeld surfaces and fingerprint plots of the **HB1** aggregate in **1 $\alpha$**  (top) and **1 $\beta$**  (bottom). Structural data from single crystal neutron diffraction at room temperature published by Coppens and Sabine.<sup>11c</sup> Normalized external distances ( $d_{\text{norm}}$ )<sup>27</sup> are plotted on the surface, with standard colour scale from Crystal Explorer.<sup>29</sup>

The similarities between the first coordination sphere of  $\alpha$  and  $\beta$  are also evident from the analysis of the Hirshfeld surface fingerprints of the **HB1** aggregate in the two structures, see Figure 2. In particular the fingerprints at shorter internal/external distances from the surface are basically identical, with the typical double horn feature caused by HB donor and acceptor contacts, whereas at larger values they somewhat differ. The two Hirshfeld surfaces are very similar in the oxalic acid part, but of course the shape around the two water molecules is different.

As we have recently communicated,<sup>19</sup> a proton migration has been observed in **1a** at high pressure. The evidence for this came from structures determined by X-ray diffraction: as the pressure is increased, all the C-O distances of the oxalic acid molecule become very similar at values intermediate between those typical of single and double bonds. This suggested the formation of two COO<sup>-</sup> groups instead of the more familiar COOH and therefore a transformation of the oxalic acid molecule into an oxalate di-anion. Because the positions of H atoms are quite difficult to determine based on the X-ray data only, quantum chemical calculations were carried out at the density functional level with periodic boundary conditions (P-DFT), to simulate the full crystal structures of **1a** under different compression conditions. These calculations indicated that two structures are competing on the potential energy surface (PES) with one corresponding to a *neutral* (N) and the other to a *charge transfer* (CT) configuration. The CT structure is located on the PES above 0.5 GPa and it is characterized by a proton shift and therefore the ions (C<sub>2</sub>O<sub>4</sub>)<sup>2-</sup> and (H<sub>3</sub>O)<sup>+</sup> are observed. At low pressures, the N form is more stable than the CT form, in terms of electronic energy, enthalpy and free energy. However, the CT structure takes advantage of a smaller volume (see Figure 3) and therefore its enthalpy becomes progressively smaller than that of the N configuration (Figure 4). In addition, the PES is substantially modified upon compression and, above 6 GPa, it is no longer possible to find a minimum corresponding to the N configuration.

The neutron diffraction experiments, carried out on a deuterated powder sample, allow us to confirm the preliminary X-ray observation, besides using a different isotope, which is mandatory for the neutron diffraction experiments. Deuterium does not change much the structure, but simply gives a slightly weaker HB and therefore a slightly looser packing, see the comparison between unit cell volumes from neutron diffraction data on deuterated sample and X-Ray diffraction data on hydrogenated sample in Figure 3.

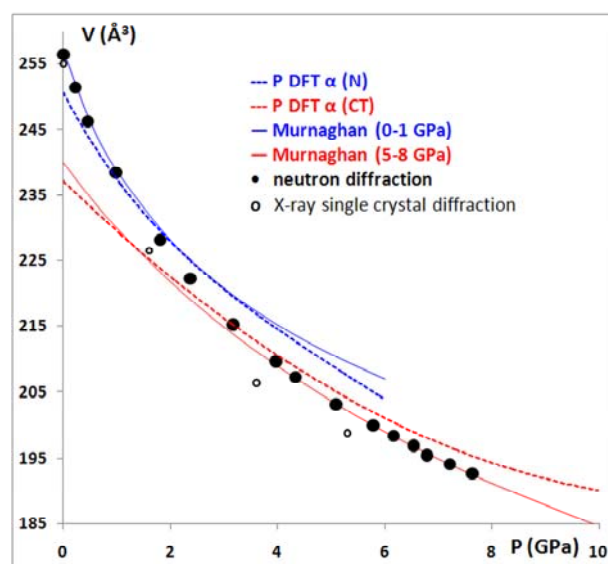


**Figure 3** Equation of state of **1a**: results of experimental neutron powder diffraction and single crystal X-ray diffraction are reported together with the P-DFT predictions for N and CT configurations. Two separate Murnaghan<sup>30</sup> equation of states were refined using neutron data in the ranges 0-1 and 5-8 GPa ( $V_0 = 257.2(5)$  and  $239.9(13)$  Å<sup>3</sup>;  $K_0 = 9.7(13)$  and  $21.6(9)$  GPa respectively).

It is interesting to examine the intermolecular geometries. In Table 1, the predicted geometries of **HB1** aggregate are reported for N and CT configurations of **1a** and **1b**, together with neutron diffraction results on the deuterated species. Along the pressure range, a pronounced elongation of the O2-H21 bond is predicted for the **1a** N configuration, from 1.04 Å up to 1.13 Å (at 6 GPa). On the other hand, in the **1a** CT form the O3-H21 distance decreases from 1.10 Å to 1.06 Å (at 10 GPa). Both results indicate that high pressure stabilizes the CT configuration. It is important to point out that N or CT are idealized configurations, whereas the observed or computed structures are the result of a mixing. It is natural to associate each structure with the dominant configuration, based on the geometry. However, the O2-H21 elongation or the O3-H21 shortening tell us that the mixing is sensitive to compression, and for both structures the contribution of CT increases.

**Table 1** Main features of the HB1 geometries of **1a** and **1b** at selected pressures. Theoretical calculations are for the hydrogenated phase at 0K. X-ray diffraction data and neutron diffraction data on deuterated species are also tabulated.

Phase	Pressure (GPa)	O2---O3 Å	O2-H21 Å	H21---O3 Å
<b>1a (expt)</b>	0.0001 <sup>(a)</sup>	2.524(2)	1.031(2)	1.493(2)
	0.0001 <sup>(b)</sup>	2.494(4)	-	-
	1.6 <sup>(b)</sup>	2.449(5)	-	-
	1.8 <sup>(c)</sup>	2.51(2)	1.05(2)	1.46(2)
	3.6 <sup>(b)</sup>	2.429(4)	-	-
	4.3 <sup>(c)</sup>	2.47(2)	1.20(2)	1.27(2)
	5.3 <sup>(b)</sup>	2.423(17)	-	-
	6.2 <sup>(c)</sup>	2.46(1)	1.30(2)	1.16(2)
<b>1a(N)</b>	0.0001	2.513	1.043	1.471
	0.5	2.502	1.046	1.458
	2.0	2.472	1.058	1.415
	4.0	2.443	1.075	1.369
	6.0	2.401	1.130	1.271
<b>1a(CT)</b>	0.5	2.426	1.325	1.102
	2.0	2.438	1.364	1.077
	4.0	2.436	1.372	1.069
	6.0	2.429	1.368	1.068
	8.0	2.426	1.371	1.062
	10.0	2.421	1.370	1.060
<b>1b (expt)</b>	0.0001 <sup>(a)</sup>	2.538(2)	1.02(2)	1.520(2)
<b>1b(N)</b>	0.001	2.517	1.029	1.495
	0.5	2.511	1.031	1.487
	2.0	2.495	1.035	1.464
	4.0	2.482	1.034	1.453
	6.0	2.470	1.035	1.440
	8.0	2.459	1.038	1.425
	10.0	2.450	1.038	1.415
<b>1b(CT)</b>	0.5 <sup>(d)</sup>	2.469	1.417	1.055
	2.0 <sup>(d)</sup>	2.460	1.409	1.055
	4.0	2.443	1.378	1.069
	6.0	2.443	1.385	1.064
	8.0	2.441	1.387	1.061
	10.0	2.438	1.388	1.058

<sup>(a)</sup> From the single crystal neutron diffraction data on deuterated samples, see Coppens et al.<sup>11c</sup>

<sup>(b)</sup> From single crystal X-ray diffraction, see Casati *et al.*<sup>19</sup>

<sup>(c)</sup> From neutron powder diffraction on deuterated samples, this work.

<sup>(d)</sup> this CT phase can be considered as a different phase respect to that stable in the regime 3-10 GPa (reported in the following entries), based on the computed volume, compressibility and geometry.

The refinements of the neutron diffraction data confirm the shift of the acidic hydrogen, although it is not possible to ascertain whether a continuous migration or instead a discontinuous phenomenon occurs. This is due in part to the inherent lower accuracy of refinements against powder data, here augmented by the noise of a high pressure cell, and in part to the thermal vibration of the hydrogen atom, which does not allow us to distinguish unambiguously between a single atomic site and two very close disordered sites.

At variance from the atomic positions, the unit cell constants are quite accurately measured by powder diffraction

techniques (Supporting Information†). A comparison with the theoretical predictions is therefore possible (Figure 3): at low pressure the observed unit cell data are quite close to those predicted for the N configuration, whereas at high pressure they are quite close to the CT one. An intermediate region is found between 2 and 4 GPa.

If we fit two different equations of state,<sup>30</sup> one for data in the pressure range 0-1 GPa and another in the pressure range 5-8 GPa, we obtain two functions quite close to those predicted for the N and the CT configurations (see Figure 3). Thus, analysis of unit cell parameters seems to confirm that a progressive phase change occurs, in agreement with the theoretical predictions.

It is therefore interesting that the two electronic configurations which contribute to the covalent component of the HB (scheme 1) can be interchanged as a function of the pressure applied on the system. As anticipated in a previous communication, the mechanism of the proton shift takes advantage of the so-called anti-cooperative effect.<sup>31</sup> Namely, the two weaker (softer) HB's in which water acts as a donor (see Figure 1), are the most compressible. This produces a small but significant elongation of O3-H31 and O3-H32 bond distances, hence a substantial repolarization of the water molecule. The more negative O atom becomes a much better HB receiver and therefore the CT configuration is stabilized.

The neutron diffraction results in Table 1 show that **1a** deviates from the expected trend of a neutral configuration under compression. Very likely, the structure refinements of data collected between 2 and 6 GPa are affected by disorder between the geometries of the two configurations. It is also clear that at the highest pressure (6.2 GPa) the deuterium shift is not yet complete, because the O3-H21 distance remains significantly longer than expected for a "pure" CT configuration at the same pressure (1.16 vs 1.07 Å). We have to consider, however, that the deuterated species of **1a** is characterized by a weaker HB, compared to the hydrogenated species: see for example the longer O2---O3 distance. As a matter of facts, based on C-O distances, the accurate X-ray diffraction data on **1a** were consistent with an almost completed proton shift at 5.3 GPa. Indeed an excellent agreement between X-ray diffraction data and CT configuration is found for the O2---O3 distance. The deuterated **1a** form attains equilibrium at a slightly larger volume compared to hydrogenated form and this explains the higher pressure necessary to induce the N → CT conversion.

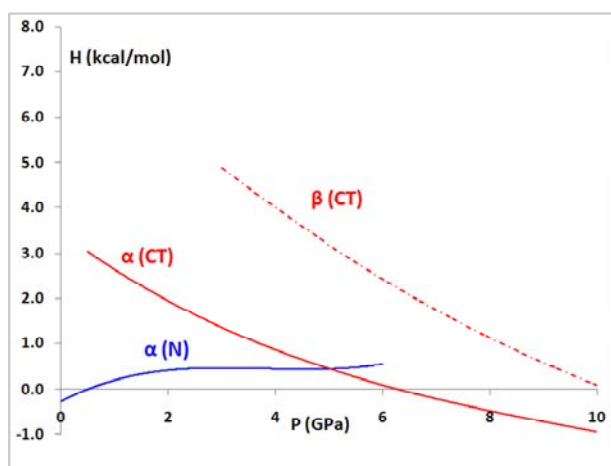


**Figure 4** Relative enthalpies per unit cell of the various phases of **1** as a function of the pressure. At each pressure, enthalpies are scaled respect to  $\beta$  (N), which is stable over the whole range. Note that in the range 0-2 GPa, a substantially different  $\beta$  CT configuration is computed at quite high energies, but it is not reported in this graph.

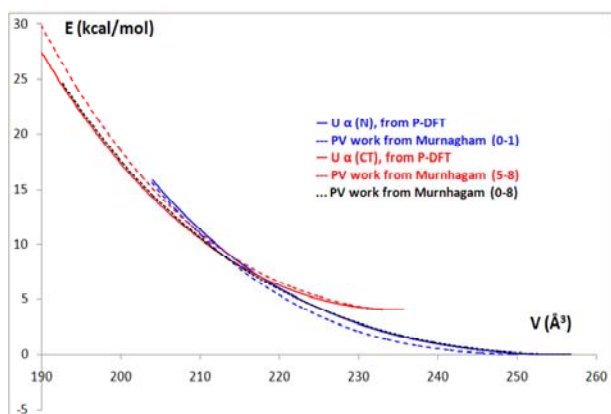


**Figure 5** The PV work (per unit cell) as a function of the unit cell volume, computed from the equation of states derived from neutron diffraction data on **1a** and the internal energies  $U$  computed for the N and CT configurations, with Deuterium isotopes. Murnaghan (0-8) work is computed from the equation of state refined using all experimental unit cell volumes from neutron diffraction experiments, in the range 0-8 GPa. Murnaghan (0-1) and Murnaghan (5-8) works come from the two equation of states refined using only unit cell volumes in the 0-1 GPa and 5-8 GPa ranges, respectively. All energies are scaled respect to the phase more stable at room pressure.

Both P-DFT calculations and experimentally determined equation of states allow us to estimate how much energy the system requires in order to complete the transformation (see Figure 5). Using the Landau–Lifshitz relation,<sup>32</sup> the work done on the system is easily calculated from experimental volumes and pressure, under the approximation of hydrostatic and reversible conditions. Apart from the heat exchanged ( $-TdS$ ), this should correspond to the variation of internal energy. Indeed, the agreement is qualitatively and also quantitatively very good (see Figure 5). PV work was computed from the Murnaghan<sup>30</sup> equation of state on all experimental data, or otherwise on the two separate sets, 0-1 GPa and 5-8 GPa simulating the N and CT configuration, as already shown in Figure 3. Assuming that at 6 GPa ( $V \sim 200 \text{ Å}^3$ ) the transfer is complete, and that all the work is spent to move the hydrogens, then an energy of ca. 4 kcal/mol per each HB is

computed (it is ca. 16 kcal per unit cell and there are 4 strong HBs per unit cell).

Given the similar packing motif, it is interesting making a comparison between **1a** and **1b** and test whether a proton transfer is possible in this case as well. Interestingly, we found some features for the **1b** form which are clearly at variance with the behaviour of **1a**.

The neutral configuration of **1b** is always stable over the pressure range 0-10 GPa. As noted above, **1b** was always observed as deuterated sample. **1a** and **1b** have very similar free energies, **1b** being associated with a more favourable entropic term, thus it would be expected more stable at higher temperatures. On the other hand, the relative stability of deuterated or hydrogenated species is very similar. We might therefore conclude that observation of **1b** depends more on the crystallization conditions, for example  $D_2O$  instead of  $H_2O$ .

While at room conditions, the HB1 geometries of **1a** and **1b** are quite similar (O-H = 1.04 / 1.03 Å; O---O = 2.51 / 2.52 Å), the neutral configuration of **1b** is not particularly sensitive to the compression: the acidic protons remain attached to oxalic molecule with only minor elongation of the O-H distances. Thus, C-O bonds remain single and double, with a small progressive contraction of both distances. This behaviour is explained by the orientation of the water molecules in the two forms. In **1a**, the stereochemistry is optimal to enhance the covalent contributions because the water lone pairs are properly oriented toward the oxalic acid protons. In **1b** this is different, as one can see from Figure 1.

A CT configuration was also computed for the  $\beta$  form. Actually, we observe a discontinuous behaviour with one CT configuration in the low pressure regime and at quite a high energy with respect to the N configuration. Above 3 GPa, a minimum corresponding to a different CT structure was found, which remains stable upon further compression and for which the enthalpy difference with respect to the N configuration decreases as a function of  $P$ . Interestingly, at high pressure, the CT configurations of **1a** and **1b** are quite similar and their energies become also quite close. However, it is not possible to find a clear relation between their metrics and no common supercell could be found, within a determinant limit of 8. In Figure 6, the Hirshfeld surfaces and fingerprints of the HB1 aggregates of the two CT forms are displayed. The simulated X-ray powder diffraction spectrum (Supporting Information†) also indicates that these two structures are not identical.

One of the main features of both **1a** and **1b** HP CT structures is the symmetrisation of the hydronium cation. In fact, the three O3-H distances become quite similar, as well as the corresponding HB's. Therefore, while at room conditions HB1 is clearly a stronger aggregate interconnected with the others by weaker HB's of the water protons, at high pressure instead one cannot identify an aggregate as the three strong HB's generate a 3D network. The symmetrisation of the hydronium also implies a (imperfect) threefold arrangement around the cation. The "imperfection" is due to one HB being actually bifurcated, see Figure 8. This is also quite visible from the Hirshfeld surfaces in Figure 6.

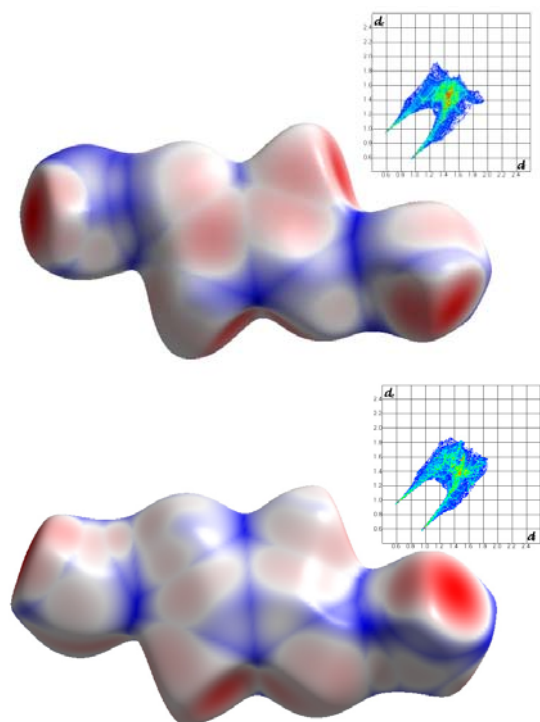


**Figure 6** Hirshfeld surfaces and corresponding fingerprints of the **HB1** aggregate in the  $\alpha$  (top) and  $\beta$  (bottom) form of oxalic acid di-hydrate at  $V = 185 \text{ \AA}^3$ . Structural data are from geometry optimization of the CT configurations. Normalized external distances are plotted on the surface, with standard colour scale from Crystal Explorer.<sup>29</sup>

10

The different behaviour of **1 $\alpha$**  and **1 $\beta$**  upon compression can be visualized by scanning a vibration mode involving the acidic proton H21. A  $B_u$  type mode was selected with harmonic frequency in the range  $2000\text{--}2700 \text{ cm}^{-1}$ , being quite

15

self trapped in the HB system – see Figure 7. Note that the harmonic approximation gives a quite large overestimation of the actual vibration frequencies when highly anharmonic modes are concerned, as it was reported by Mohaček-Grošev *et al.*<sup>33</sup> for **1 $\alpha$**  at room pressure.

20

The O2-H21 elongation occurring in **1 $\alpha$ (N)** is quite visible, as well as the H21-O3 contraction in **1 $\alpha$ (CT)**. On the other hand the position of the minima of both **1 $\beta$**  configurations is not much altered by the pressure. This feature is very important because it anticipates that a larger barrier is associated with

25

the  $N \rightarrow CT$  conversion of **1 $\beta$** .

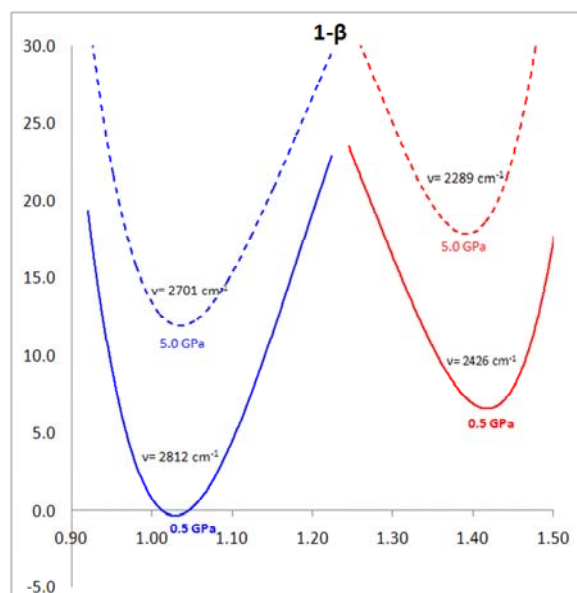
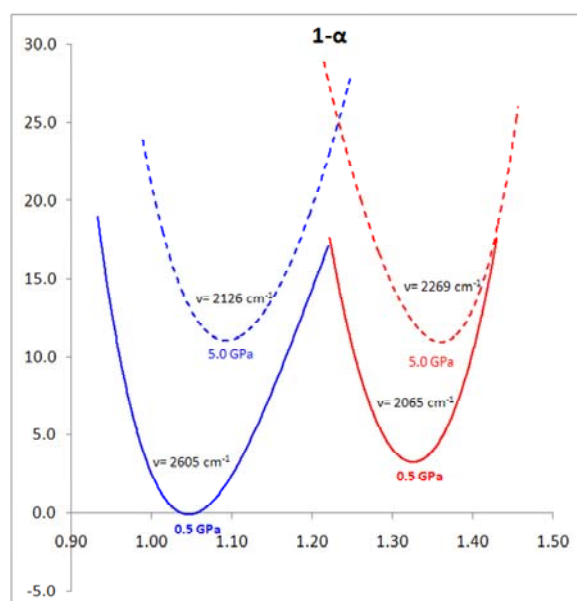


**Figure 7** The enthalpy (kcal/mol) per unit cell at 0.5 and 5 GPa scanned along one of the O2-H21 stretching modes (O2-H21 distance in Å is given in abscissa). Top **1 $\alpha$** , bottom **1 $\beta$**  forms. Blue curves correspond to structures in N configuration and red curves to the CT configurations. At each pressure, energies are scaled respect to **1 $\alpha$**  N form, whereas the gap between 0.5 GPa and 5.0 GPa curves is chosen to optimize the graphics, as it exceeds 100 kcal/mol. At 10 GPa, the positions of the minima for **1 $\beta$**  are almost unchanged.

30

35

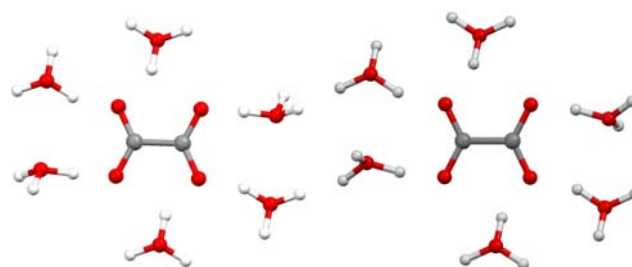


**Figure 8** Calculated CT geometries of **1 $\alpha$**  (left) and **1 $\beta$**  (right) at 10 GPa. Note the bifurcated HB given by two hydronium cations. This picture also shows the great similarity between the two CT structures

40

## Conclusions

P-DFT calculations and neutron diffraction data show that high pressure is able to stabilize a structure associated with higher energy at room conditions. This is particularly relevant for chemical bonds formed by the resonance of two or more electronic configurations, as is the case for strong hydrogen bonds.

For the  $\alpha$  form of oxalic acid di-hydrate, all experimental and theoretical evidences indicate that, as the pressure is increased, the acidic protons migrate toward the water molecules. Thus, the di-hydrated co-crystal transforms into a di-hydronium oxalate salt. Indeed, this reminds us of the original discussion on the nature of this species.<sup>9</sup> Theoretical calculations predict that this mechanism is originated by the equilibrium between two structures, the N and CT ones.

On the other hand, the different stereochemistry of the  $\beta$  polymorph hampers the same transformation, which is not predicted to occur within the range 0-10 GPa. In fact, at high pressure **1 $\beta$ (N)** is always stable on the PES, at variance from **1 $\alpha$ (N)** which “disappears” above 6 GPa. Instead, in **1 $\beta$**  the CT configuration requires more external work to be stabilized. Moreover, another important feature hampers the transformation, namely the height of the interconversion barrier. In fact, because the two geometries are much further apart, an intermediate between N and CT must be associated with a higher energy.

The compression of a solid raises its internal energy, because of the increased atom-atom or molecule-molecule repulsions. However, this may also modify the PES landscape. As a result, otherwise less favourable electronic configurations may become accessible and even dominating, as it is the case for oxalic acid di-hydrate. Several other HB systems, for example most of compounds with carboxylic groups, could behave in this way although not yet investigated. Amino acids in solids are already in CT (zwitter ionic) configuration even at room pressure, whereas most of them are in neutral configuration in the gas phase. The pressure should therefore further stabilize the zwitter ionic form.

Further research on similar species could shed more light on the proton shift mechanism and allow more detailed explanation of the material properties.

## Notes and references

<sup>a</sup>Department of Chemistry and Biochemistry, University of Bern, Freiestrasse 3, CH 3012, Bern Switzerland; <sup>b</sup>Diamond Light Source Ltd., Harwell Science and Innovation Campus, Didcot, Oxfordshire OX11 0DE; <sup>c</sup>ISIS Neutron Facility, STFC Rutherford Appleton Laboratory, Harwell Science and Innovation Campus, Didcot, Oxfordshire, OX11 0QX; <sup>d</sup>Department of Structural Chemistry and Inorganic Stereochemistry, University of Milan, via Venezian 21 20133 Milano Italy  
E-mail: [piero.macchi@pcb.unibe.ch](mailto:piero.macchi@pcb.unibe.ch)

† Electronic Supplementary Information (ESI) available: results of the neutron diffraction data and simulated X-ray powder diffraction files of relevant phases discussed in the paper; theoretical unit cell data for **1 $\beta$** . This work was supported by the Swiss National Science Foundation, project 200021\_126788/1. We thank ISIS and the STFC for the provision of neutron beam time and D.J. Francis for his technical assistance during the neutron diffraction experiment.

<sup>60</sup> § Promolecule and procrystal density are obtained by summation of the electron densities of the isolated, spherical atoms.

§ For larger unit cell volumes the wave function was stable even without any mixing, but of course all calculations were eventually carried out with the 20% mixing (to properly compare the electronic energies). Anyway, no significant difference in the optimized geometries was observed between 0%, 10% or 20% mixing.

- 1 W.M. Latimer, W.H. Rodebush, *J. Am. Chem. Soc.* 1920, **42**, 1431.
- 2 G.N. Lewis, *Valence and Structure of Atoms and Molecules*, Chemical Catalog, New York, 1923.
- 3 M. L. Huggins, *J. Org. Chem.* 1936, **1**, 407-456
- 4 L. Pauling, *The Nature of the Chemical Bond and the Structure of Molecules and Crystals*, 3rd ed., Cornell University Press, Ithaca, NY, 1960.
- 5 P. Gilli, G. Gilli, *J. Mol. Struct.* 2000, **552**, 115.
- 6 G. K. H. Madsen, G. J. McIntyre, B. Schött, F. K. Larsen, *Chem. Eur. J.* 2007, **13**, 5539-5547.
- 7 P. H. R. Groth, *Chemische Kristallographie. Fünfter teil*; Engelmann: Leipzig, 1910; pp 136-137.
- 8 A. C. R. Villiers, *Hebd. Seances Acad. Sci.* 1880, **90**, 821.
- 9 a) J.I. Robertson, I.J. Woodward, *Chem Soc.* 1936, 1817; b) R. Brill, C. Hermann, A. Peters, *Ann. Phys. Lpz.*, 1942, **42**, 357; c) A.D. Booth, *Proc. Roy. Soc. A* 1947, **190**, 490.
- 10 F.R. Ahmed, D.W. Cruickshank, *Acta Cryst.* 1953, **6**, 385-392.
- 11 a) F. F. Iwasaki, H. Iwasaki, Y. Saito, *Acta Cryst* 1969, **23**, 64; b) T. M. Sabine, W. G. Cox, B. M. Craven, *Acta Cryst* 1969, **B25**, 2437; c) P. Coppens, T. M. Sabine, *Acta Cryst* 1969, **B25**, 2442; c) a) A. Lehmann, P. Luger, C. W. Lehmann, R. M. Ibberson, *Acta Cryst.*, 1994, **B50**, 344, b)
- 12 (a) D. Zobel, P. Luger, W. Dreissig, T. Koritsanszky, *Acta Cryst.* 1992, **B48**, 837; (b) Wang, C. J. Tsai, W. L. Liu, L. D. Calvert, *Acta Cryst.* 1985, **B41**, 131.
- 13 H. Iwasaki, Y. Saito, *Acta Cryst.*, 1964, **17**, 1472.
- 14 F. H. Allen, O. Kennard, *Chem. Des. Autom. News*, 1993, **8**, 31.
- 15 M. Wenger, J. Bernstein, *Mol. Pharmaceutics*, 2007, **4**, 355.
- 16 For example a) A. Katrusiak, R.J. Nemes, *J. Phys. C*, 1986., **19** L765; b) A. Katrusiak *Acta Cryst*, 1990, **B46**, 246; c) M. Walker, C.R. Pulham, C.A. Morrison, D.R. Allan, W.G. Marshall, *Phys. Rev. B*, 2006, **73**, 224110; d) E.V. Boldyreva, *J. Mol. Struct.*, 2004, **700**, 151.
- 17 M. L. Putkonen, R. Feld, C. Vettier, M. S. Lehmann, *Acta Cryst.*, 1985, **B41**, 77.
- 18 W.G. Marshall, C.R. Pulham, D.R. Allan, *ISIS experimental report*, RB Nr. 14428.
- 19 N. Casati, P. Macchi, A. Sironi *Chem. Comm.*, 2009, 2679.
- 20 W.G. Marshall, D.J. Francis *J. Appl. Cryst.* 2002, **35**, 122.
- 21 a) A. Z. Kuznetsov, V. Dmitriev, L. Dubrovinsky, V. Prakapenka, H.-P. Weber *Solid State Comm.* 2002, **122**, 125, b) R. A. Miller, D. E. Schuele *J. Phys. Chem. Solids*, 1969, **30**, 589, c) D. L. Waldorf, G. A. Alers, *J. Appl. Phys.*, 1962, **33**, 3266.
- 22 A. A. Coelho Topas-R, Version 4: General profile and structure analysis software for powder diffraction data; Bruker AXS: Karlsruhe, Germany, 2006
- 23 J. D. Barnett, C.D. Bosci, *J. Appl. Phys.*, 1969, **40**, 3144.
- 24 R. Dovesi, V.R. Saunders, C. Roetti, R. Orlando, C. M. Zicovich-Wilson, F. Pascale, B. Civalleri, K. Doll, N.M. Harrison, I.J. Bush, Ph. D'Arco, M. Llunell CRYSTAL09 User's Manual, University of Torino, Torino, 2009.
- 25 a) A. D. Becke, *J. Chem. Phys.*, 1993, **98**, 5648. b) C. Lee, W. Yang, R. G. Parr, *Phys. Rev. B*, 1988, **37**, 785.
- 26 S. Grimme *J. Comput. Chem.* 2006, **27**, 1787.
- 27 J. J. McKinnon, M. A. Spackman, A. S. Mitchell, *Acta Cryst.*, 2004, **B60**, 627; J. J. McKinnon, M. A. Spackman, D. Jayatilaka, *Chem. Comm.* 2007, 3814; M. A. Spackman, J. J. McKinnon *CrystEngComm*, 2002, **4**, 378.
- 28 S.A. Moggach, D. R. Allan, S. Parsons, L. Sawyer L. *Acta Cryst.*, 2006, **B62**, 310.
- 29 S. K. Wolff, D. J. Grimwood, J. J. McKinnon, D. Jayatilaka, M. A. Spackman *Crystal Explorer 2.1*.

- 
- 30 F. D. Murnaghan, *Am. J. Math.* 1937, **49**, 235.  
31 T. Steiner, W. J. Saenger, *J. Am. Chem. Soc.*, 1992, **114**, 7123.  
32 L. D. Landau, E. M. Lifshitz *Theory of elasticity*. Elsevier 1986.  
33 V. Mohaček-Grošev, J. Grdadolnik, J. Stare, D. Hadži *J. Raman Spectrosc.*, 2009, **40**, 1605.